Acta Crystallographica Section B
**Structural Science**
ISSN 0108-7681

# Molecular and crystalline structure of cycloheptanespiro-3′(4′*H*)-6′,7′,8′,9′-tetrahydrocyclohexa[*b*][1,4]thiazole-2′(5′*H*)-thione from powder synchrotron X-ray diffraction data

**Edward E. Avila,[a] Asiloé J. Mora,[a]* Gerzon E. Delgado,[a] Ricardo R. Contreras,[b] Andrew N. Fitch[c] and Michela Brunelli[c]**

[a]Laboratorio de Cristalografía, Departamento de Química, Facultad de Ciencias, Universidad de Los Andes 5101, Venezuela, [b]Laboratorio de Organometálicos, Departamento de Química, Facultad de Ciencias, Universidad de Los Andes 5101, Venezuela, and [c]European Synchrotron Radiation Facility, BP 220, F-38043 Grenoble CEDEX, France

Correspondence e-mail: asiloe@ula.ve

Received 10 August 2007
Accepted 3 January 2008

A series of bidentate nitrogen–sulfur pro-ligands has been designed and synthesized with the purpose of introducing a structural modification that favours the tetrahedral site distortions of metalloprotein systems with metallic centers surrounded by ligands containing two N atoms and two S atoms as donor groups. Some of these new pro-ligands were obtained only as powders. Here we present the molecular and crystalline structure of cycloheptanespiro-3′(4′*H*)-6′,7′,8′,9′-tetrahydrocyclohexa[*b*][1,4]thiazole-2′(5′*H*)-thione (I) solved and refined from powder synchrotron X-ray diffraction data. Two independent molecules comprising a total of 36 non-H atoms were obtained from the direct-methods solution and refined against the powder X-ray diffraction data using the Rietveld method. The molecular conformations of the heterocyclic benzothiazine ring, the fused heptenyl ring and the heptanyl spiro ring are thoroughly discussed and compared with VASP theoretical calculations and other related structures. The packing of molecules in (I) is based on hydrogen bonds of the type N—H···S and hydrophobic C—H interactions.

## 1. Introduction

Biomimetic inorganic chemistry is concerned with the synthesis and detailed electronic and structural characterization of model molecules that approach one or more properties of a protein-active metal site (Holm & Solomon, 2004). Composition, ligand type, site topology and oxidation state are among the properties that can be duplicated. In particular, efforts have been made (Solomon *et al.*, 2004; Halcrow & Christou, 1994; Malachowski *et al.*, 1999; Karlin *et al.*, 1997) to reproduce the pseudo-tetrahedral coordination spheres of metal ions linked with pro-ligands containing two N atoms and two S atoms as donor groups, since biological systems use this type of environment in the coordination of metal ions such as $Cu^{II}$ in plastocyanin or azurin (Roat-Malone, 2002), $Ni^{II}$ in nickel-hydrogenase (Kain & Schwederski, 1994) and $Zn^{II}$ in the so-called zinc finger proteins involved in the activation and regulation of the DNA transcription (Auld, 2001). Recently, Contreras *et al.* (2001, 2005, 2006) modifed the reaction conditions proposed by Bordás *et al.* (1972) in their seminal synthetic studies and synthesized a series of nitrogen–sulfur pro-ligands. The aim of the study was to investigate the geometry and steric effects of the chelate formation of the new pro-ligands with the various biometals responsible for biological activity in metalloproteins. Some of the [NS] pro-ligands have only been obtained as powders. Here we discuss the molecular and crystal structure of cycloheptanespiro-3′(4′*H*)-6′,7′,8′,9′-tetrahydrocyclohexa[*b*][1,4]thiazole-2′(5′*H*)-thione,

**Table 1**
Experimental details.

| | |
|---|---|
| Crystal data | |
| Chemical formula | $C_{15}H_{23}NS_2$ |
| $M_r$ | 281.48 |
| Cell setting, space group | Monoclinic, $P2_1/c$ |
| Temperature (K) | 298 |
| $a, b, c$ (Å) | 13.11563 (4), 21.32201 (6), 11.75591 (3) |
| $\beta$ (°) | 113.9899 (1) |
| $V$ (Å$^3$) | 3003.57 (2) |
| $Z$ | 8 |
| $D_x$ (Mg m$^{-3}$) | 1.245 |
| Radiation type | Synchrotron |
| $\mu$ (mm$^{-1}$) | 1.99 |
| Specimen form, colour | Cylinder (particle morphology: thin powder), yellow |
| Specimen size (mm) | 40.0 × 1.5 × 1.5 |
| Specimen preparation temperature (K) | 298 (1) |
| Data collection | |
| Diffractometer | Inet ID31, ESRF, Grenoble, France |
| Data collection method | Specimen mounting: borosilicate glass capillary; mode: transmission; scan method: step |
| $2\theta$ (°) | $2\theta_{min}$ = 3.00, $2\theta_{max}$ = 65.96, increment = 0.003 |
| Refinement | |
| Refinement on | Intensities |
| $R$ factors and goodness-of-fit | $R_p$ = 0.050, $R_{wp}$ = 0.061, $R_{exp}$ = 0.025, $S$ = 2.51 |
| Wavelength of incident radiation (Å) | 1.25248 (3) |
| Excluded region(s) | None |
| Profile function | Pseudo-voigt |
| No. of parameters | 293 |
| H-atom treatment | Constrained |
| $(\Delta/\sigma)_{max}$ | 0.07 |

Computer programs used: *GSAS* (Larson & Von Dreele, 2007), *EXPO*2004 (Altomare *et al.*, 2004), *EXPGUI* (Toby, 2001), *PLATON* (Spek, 1990), *DIAMOND*2.1 (Brandenburg, 2001).

which was determined using synchrotron powder diffraction data.

## 2. Experimental

### 2.1. Synthesis of cycloheptanespiro-3′(4′*H*)-6′,7′,8′,9′-tetrahydrocyclohexa[*b*][1,4]thiazole-2′(5′*H*)-thione (I)

Compound (I) was synthesized from cycloheptanone (25 ml, 200 mmol; Aldrich, 99%) dissolved in a solution of $NH_4OH$ 29% v/v (Sigma-Aldrich, ≥ 97%) at a temperature of 273 K. After 10 min $CS_2$ (29 ml, 300 mmol), previously purified as described elsewhere (Gordon & Ford, 1972), was added with continuous agitation for 24 h at a temperature of 268 K. The solvent was evaporated under vacuum until a yellow crystalline powder was obtained. Yield of the overall reaction: 12.13 g (23%). The diagram shows the synthetic route of (I). Rectangular microcrystals were obtained by evaporation of the recrystallization solvent (3:1 acetone, Fluka, ≥ 99.5%): water; m.p. 472–473 K. Mass spectroscopy (MS) data using electronic ionization showed P+, $m/z$ (I %): $C_{15}H_{23}NS_2$, 281.25 (15%). FT-IR spectra on a KBr pellet (3% p/p) gave the following bands: $\nu$ (cm$^{-1}$) ($\nu_a/\nu_s$= asymmetric/symmetric absorption bands, s = strong, m = medium, w = weak, bb = broad) $\nu$(N—H); $\nu_a$(C═C) + $\nu_a$(C═N); $\nu_s$(C═C); $\nu_s$(C═N) + $\upsilon_a$(C═S); $\nu_a$(S—CH$_2$—); $\nu_a$(CSS—); $\nu_s$(CSS—): 3428(w), 2924(s), 2850(m), 1544(m), 1516(m), 1390(m), 1251(m).

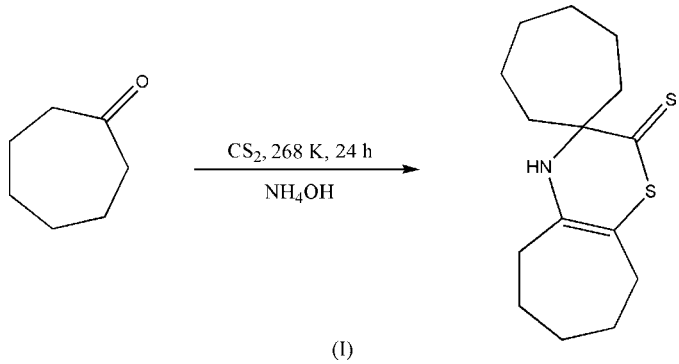


(I)

### 2.2. Powder data collection

Powder X-ray diffraction data were collected with the high-resolution powder X-ray diffractometer on beamline ID31 at ESRF (Fitch, 2004), selecting X-rays from the white undulator source with wavelength 1.25248 (3) Å. Small quantities of (I) were lightly ground with a pestle in an agate mortar and introduced into a 1.5 mm diameter borosilicate glass capillary, mounted on the axis of the diffractometer and spun during measurements. Data were collected at room temperature for several hours, normalized against monitor counts and detector efficiencies, and rebinned into steps of $2\theta$ = 0.003°.

## 3. Results

### 3.1. Structural solution and refinement

The auto-indexing program *DICVOL*91 (Boultif & Louër, 1991) indexed the diffraction pattern in a monoclinic cell, with cell parameters $a$ = 13.11563 (4), $b$ = 21.32201 (6), $c$ = 11.75591 (3) Å, and $\beta$ = 113.9899 (1)° (refined) and figures-of-merit $M_{21}$ = 102.7 (de Wolff, 1968) and $F_{21}$ = 441.2 (0.0016, 29) (Smith & Snyder, 1979). Systematic absences unequivocally assigned the space group as $P2_1/c$ (No. 14). The cell volume suggested that there were two independent molecules of (I) within the asymmetric unit. The extraction of 2021 unique reflections in the $2\theta$ range 3.00–65.96° from the powder diffraction data by the Le Bail method (Le Bail *et al.*, 1988) and the crystalline structure solution by direct methods were carried out using the routines implemented in the program *EXPO*2004 (Altomare *et al.*, 2004). All 36 non-H atoms from the two independent molecules were found in the best E-map. The model was refined by the Rietveld method (Rietveld, 1969) using the program *GSAS* (Larson & Von Dreele, 2007). The H atoms were placed in calculated positions with restricted geometries using the HFIX command of the program *SHELXL* (Sheldrick, 2008). The peak shapes were modeled using the pseudo-Voigt peak-shape function (Thompson *et al.*, 1987), which included the axial divergence correction at low angle (Finger *et al.*, 1994) and the anisotropic

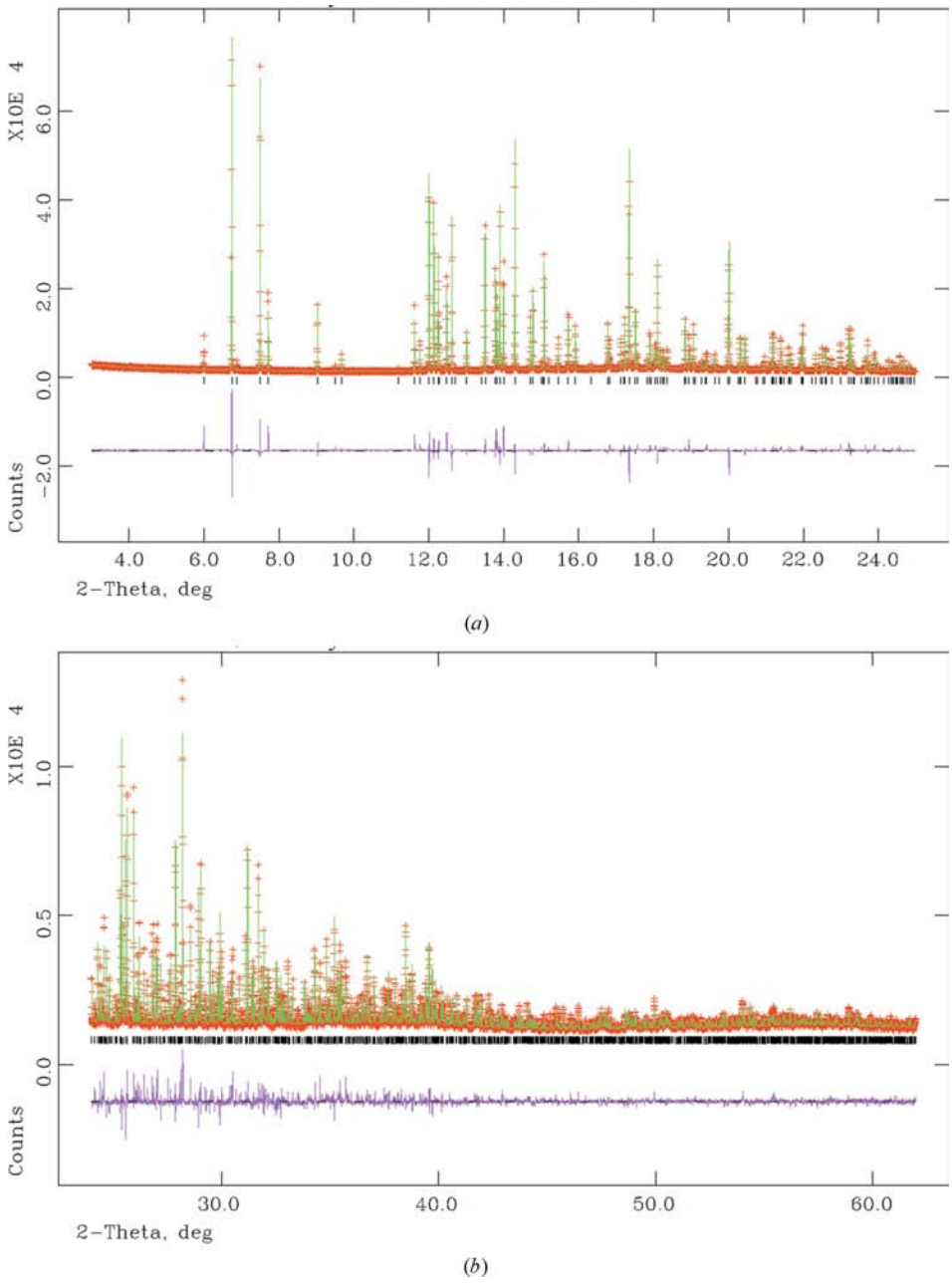


**Figure 1**
Final observed (points), calculated (lines) and difference profiles for the Rietveld refinement for (I): (*a*) low-angle data; (*b*) high-angle data.

line-shape broadening model (Stephens, 1999). Background was initially determined manually and then modeled using the Chebyschev polynomial function. In the final stages of the refinement, the diffuse scattering function 1 was used to model the background of the capillary. Weighted soft constraints on bond distances (± 0.005 Å) and angles (± 1°) were applied using the average values obtained from related structures found in the Cambridge Structural Database (CSD, Version 5.28, January 2007; Allen, 2002): one hit with the benzothiazine ring, eight hits with the cycloheptenyl ring and two hits with the cycloheptanyl ring. The isotropic displacement coefficients were refined in blocks: one $U_{iso}$ for the non-H atoms of the benzothiazine ring, one $U_{iso}$ for the remaining non-H atoms in the fused heptenyl ring and one $U_{iso}$ for the non-H atoms in the heptanyl spiro ring. Finally, the isotropic displacement coefficients of each of the H atoms were refined as 1.2 times the value of the temperature factor of their riding non-H atom. With this refinement routine, the use of the Marquardt damping factor was not necessary since the refinement was stable and convergence was readily achieved. Finally, to determine if the diffraction data contain systematic errors or if modeling of the peak shape and background was correct, a refinement without a model (Le Bail *et al.*, 1988) was conducted. The refinement produced excellent agreement factors: $R_p = 0.037$, $R_{wp} = 0.042$ and $\chi^2 = 3.014$; therefore, the above problems were ruled out. Table 1 shows experimental details for the data collection, structural solution and the Rietveld refinement.[1] The final Rietveld plot is shown in Fig. 1.

### 3.2. Solid-state *ab initio* calculations

Periodic, solid-state calculations were performed using the Vienna *ab initio* simulation package *VASP* (Kresse & Hafner, 1993; Kresse & Furthmuller, 1996). The following execution parameters were used: GGA-PBE PAW potentials (Kresse & Joubert, 1999), electronic convergence at $1 \times 10^{-5}$ eV, an optional cut-off controlling the accuracy of the calculations set to 400 eV, Davidson-blocked iterative optimization of the wavefunctions in combination with reciprocal space projectors (Davidson, 1983), a $2 \times 1 \times 2$ k-mesh for the reciprocal space integration with a Monkhorst–Pack scheme (Monkhorst & Pack, 1976), and a Methfessel–Paxton smearing with a width of 0.2 eV for energy corrections (Methfessel & Paxton, 1989). Atomic-coordinate-only optimizations of (I) were performed

[1] Supplementary data for this paper are available from the IUCr electronic archives (Reference: KD5017). Services for accessing these data are described at the back of the journal.

**Table 2**
Bond distances (Å) and angles (°).

| | XRD | | DFT-VASP | | | | |
|---|---|---|---|---|---|---|---|
| | (I) | (II) | (I) | (II) | (I) Δ (XRD-DFT) | (II) Δ (XRD-DFT) | CACHIX |
| S1—C1 | 1.692 (9) | 1.668 (6) | 1.696 | 1.695 | −0.004 | −0.027 | 1.684 (2) |
| S2—C1 | 1.722 (9) | 1.727 (8) | 1.735 | 1.744 | −0.013 | −0.017 | 1.739 (3) |
| S2—C9 | 1.830 (8) | 1.843 (6) | 1.849 | 1.856 | −0.019 | −0.013 | 1.834 (2) |
| N1—C3 | 1.37 (1) | 1.38 (1) | 1.345 | 1.339 | 0.027 | 0.045 | 1.343 (3) |
| N1—C9 | 1.451 (8) | 1.456 (8) | 1.458 | 1.461 | −0.007 | −0.005 | 1.456 (3) |
| C1—C2 | 1.449 (9) | 1.430 (8) | 1.418 | 1.412 | 0.031 | 0.018 | 1.408 (3) |
| C2—C3 | 1.381 (9) | 1.39 (1) | 1.404 | 1.408 | −0.011 | −0.027 | 1.388 (3) |
| S1—C1—S2 | 115.7 (5) | 116.5 (4) | 113.6 | 114.2 | 2.110 | 2.210 | 113.8 (1) |
| S1—C1—C2 | 124.1 (6) | 121.3 (5) | 125.0 | 124.3 | −0.890 | −2.950 | 124.5 (2) |
| S2—C1—C2 | 119.5 (6) | 121.0 (6) | 121.1 | 121.2 | −1.600 | −0.190 | 107.6 (2) |
| S2—C9—N1 | 111.0 (5) | 109.6 (6) | 107.2 | 106.6 | 3.800 | 2.990 | 121.6 (2) |
| N1—C3—C2 | 123.7 (8) | 124.2 (6) | 123.7 | 123.5 | 0.000 | 0.690 | 124.0 (2) |
| C1—S2—C9 | 101.5 (4) | 99.3 (3) | 102.7 | 101.1 | −1.170 | −1.820 | 102.8 (1) |
| C3—N1—C9 | 118.5 (6) | 120.2 (6) | 123.7 | 124.1 | −5.240 | −3.980 | 123.9 (2) |
| C1—C2—C3 | 121.9 (7) | 120.7 (7) | 121.0 | 120.8 | 0.910 | −0.110 | 121.1 (2) |

using the experimental cell parameters and atomic positions obtained from the X-ray powder diffraction Rietveld refinement. The structure was evaluated and compared with the structure obtained from X-ray powder diffraction.

## 4. Discussion

### 4.1. Molecular conformation

Fig. 2 shows the atom labeling and molecular conformation of the two independent molecules of (I) in the asymmetric unit. Selected average bond angles and distances of the benzothiazine ring (*A* in the diagram), the fused cycloalkene and spiro rings (*B* and *C* in the diagram) are shown in Table 2, which are compared with those obtained from *VASP* calculations and with the related compound 5,6,7,8-tetrahydro-4*H*-3,1-benzothiazine-2(1*H*)-spirocyclohexane-4-thione [Castiñeiras-Campos *et al.*, 1983 (CACHIX)], found in the CSD (Allen, 2002).

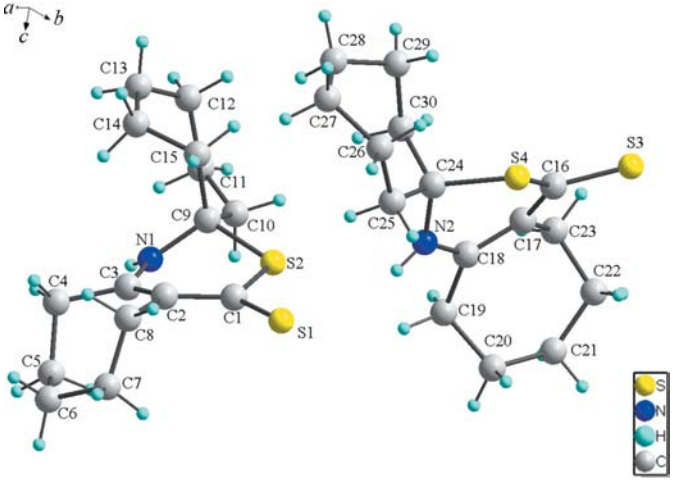


**Figure 2**
The two molecules of (I) in the asymmetric unit showing the atom labeling scheme.

The *VASP* theoretical calculations essentially show excellent agreement with the powder X-ray diffraction study. A comparison of X-ray experimental and theoretically calculated distances between covalently bonded non-H atoms in the three rings show agreement; the largest difference observed is $4.5 \times 10^{-2}$ Å. Angular discrepancies are also minimal, with the largest difference being 3°. Therefore, it can be inferred that the structure solved from X-ray powder diffraction is correct. The highest-energy occupied orbitals (just below the Fermi level) are a mixture of S, N and C *p* states.

The presence of two heteroatoms (sulfur and nitrogen) in ring *A*, and the different hybridization states of its C atoms ($sp^2$ in C1/C16, C2/C17 and C3/C18, and $sp^3$ in C9/C24), makes this ring very asymmetrical. In both independent molecules, the C—S distance [1.692 (9)/1.668 (6) Å] of the thione group, the two C—S distances of the thioester group [1.722 (9)/1.727 (8) Å and 1.830 (8)/1.843 (6) Å] and the C═C distance of the fused ring *B* [1.38 (1)/1.393 (9) Å], match those observed in CACHIX within 1 s.u. The average angles in (I) also equal those of CACHIX within 1 s.u. Only the N1—C3 distance and the C3—N1—C9 angle have deviations of 4 s.u. from both CACHIX and the theoretical calculations. The evaluation of the torsion angles around ring *A*, using the criteria of Griffin *et al.* (1984), shows the presence of a mirror plane passing through C2/C17 and C9/C24, which are out of the average ring plane by −0.19 (2) and −0.37 (1) Å, respectively; and so the benzothiazine ring adopts the conformation of a distorted boat. In the fused cycloheptenyl ring (*B*), the average distances: $Csp^2—Csp^2$ [1.39 (2) Å], $Csp^2—Csp^3$ [1.51 (2) Å], $Csp^3—Csp^3$ [1.52 (2) Å] match those average distances of eight cycloheptenyl rings {$Csp^2—Csp^2$ [1.34 (2) Å], $Csp^2—Csp^3$ [1.51 (2) Å], $Csp^3—Csp^3$ [1.52 (2) Å]} reported in the literature [Weeks *et al.*, 1984 (CILXFA); Irngartinger *et al.*, 2000 (CILXAW01); Kostermans *et al.*, 1987 (CIPCAJ); Ohlbach *et al.*, 1996 (NADVAP, NADVET and NADWUK); Senge *et al.*, 1992 (VUFSIY); Ianelli *et al.*, 1995 (ZAYJUE)]. Ring *B* adopts a chair-like conformation in which atoms C2/C17, C3/C18, C4/C19 and C8/C23 are essentially coplanar (with a maximum deviation of 0.03 Å), forming the 'back' of the chair, while atoms C4/C19, C5/C20, C7/C22 and C8/C23 (with maximal deviation 0.07 Å) are also coplanar, being the 'seat' of the chair. The spiro-cycloheptanyl ring (*C*) has $Csp^3—Csp^3$ [1.52 (8) Å] bond distances and angles [116 (7)°] which match those observed in a similar spiro seven C-atom ring [de Costa *et al.*, 1994 (SUMMUI); Mekhael *et al.*, 2004 (RAGLAN)]. Ring *C* also adopts a chair-like conformation. Atoms C11/C26, C12/C27, C13/C28 and C14/C29 are coplanar (with a maximum deviation of 0.10 Å), forming the back of the

**Table 3**
Hydrogen bonds (Å, °) in I.

| $D$—H···$A$ | $D$—H | H···$A$ | $D$···$A$ | $D$—H···$A$ |
|---|---|---|---|---|
| N1—H1···S3$^{i}$ | 0.86 (2) | 2.69 (2) | 3.450 (8) | 149 (3) |
| N2—H2···S1 | 0.86 (2) | 2.63 (3) | 3.424 (7) | 154 (4) |
| C4—H41···S3$^{ii}$ | 0.97 (2) | 2.71 (1) | 3.664 (7) | 169 (2) |
| C4—H42···S3$^{i}$ | 0.97 (2) | 2.79 (2) | 3.701 (9) | 157 (2) |
| C8—H82···S1 | 0.97 (2) | 2.80 (2) | 3.200 (9) | 106 (2) |
| C14—H141···N1 | 0.97 (2) | 2.36 (2) | 2.85 (1) | 111 (2) |
| C23—H231···S3 | 0.97 (1) | 2.72 (2) | 3.081 (9) | 103 (2) |
| C26—H261···S3$^{iii}$ | 0.96 (3) | 2.80 (2) | 3.73 (1) | 163 (2) |
| C26—H261···S3$^{iii}$ | 0.96 (3) | 2.80 (2) | 3.73 (1) | 163 (2) |

Symmetry codes: (i) $x+1, -y+\frac{1}{2}, z+\frac{1}{2}$; (ii) $-x, y-\frac{1}{2}, -z+\frac{3}{2}$; (iii) $x, -y+\frac{1}{2}, z+\frac{1}{2}$.

chair, while C11/C26, C10/C25, C15/C30 and C14/C29 are coplanar (with a maximum deviation of 0.17 Å), representing the seat of the chair.

### 4.2. Hydrogen bonds

Hydrogen bonds are summarized in Table 3. Fig. 3 shows the two independent molecules (black and white) linked by N—H···S hydrogen bonds with a donor–acceptor average distance of 3.44 (2) Å, forming extended chains along the [$\bar{5}$0,10] direction. These chains can be represented by two graph symbols according to the acceptor atom: $[C_2^2(12)]_{S1}$ and $[C_2^2(12)]_{S3}$. Moreover, the combination of the $2_1$ screw axis and the *c*-glide plane build up the entire crystal, as shown in Fig. 4. In addition to the classical hydrogen bonds, there are several weak non-classical C—H···S hydrogen bonds, which play the role of keeping the extended chains together. Finally, there is a weak intramolecular non-classical C—H···N hydrogen bond (only present in one of the molecules in the asymmetric unit), which arises from the slightly different conformations adopted by the rings in each of the molecules. Heptenyl and heptanyl rings are more flexible than smaller cyclic rings and, therefore,

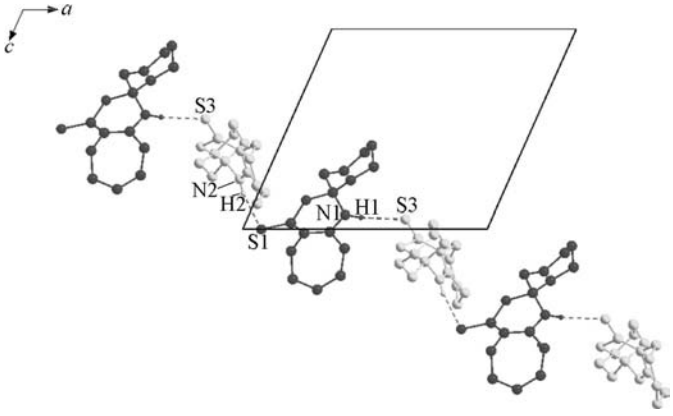


**Figure 3**
View of the extended chains of (I) linked by N—H···S hydrogen bonds running along the [$\bar{5}$0,10] direction and represented by the combination of two graph symbols: $[C_2^2(12)]_{S1}$ and $[C_2^2(12)]_{S3}$. The two independent molecules in the asymmetric unit are colored in black and white, respectively.

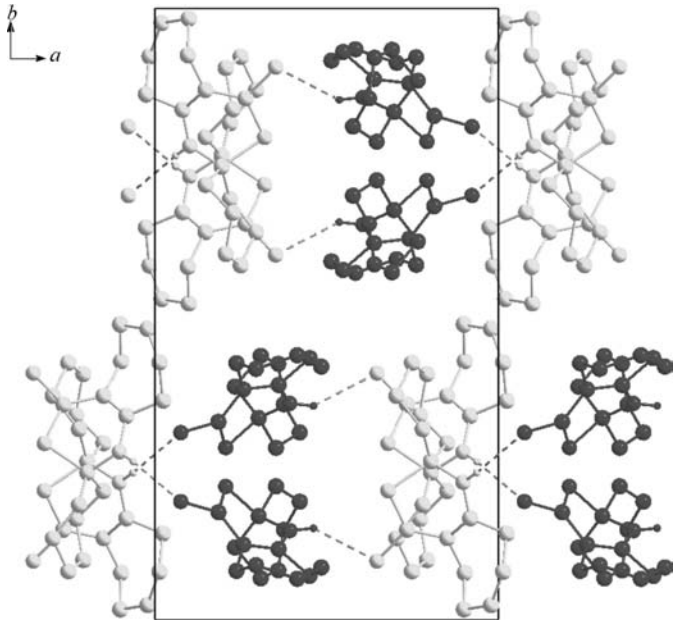


**Figure 4**
View of the parking of molecules of (I) down [001]. Black and white molecules represent the two different molecules in the asymmetric unit.

positional disorder phenomena and structures with $Z' > 1$ have been reported in the literature [de Costa *et al.*, 1994 (SUMMUI); Ohlbach *et al.*, 1996 (NADWUK); Schulze *et al.*, 2002 (AFUPAS); Albov *et al.*, 2004 (ATUYAP); Amitina *et al.*, 2004 (DANGOP); Ianelli *et al.*, 1995 (ZAYJUE); Zhang *et al.*, 1993 (HABROR)].

### 4.3. Summary

Using synchrotron powder diffraction data the structure of the compound cycloheptanespiro-3′(4′*H*)-6′,7′,8′,9′-tetrahydrocyclohexa[*b*][1,4]thiazole-2′(5′*H*)-thione (I) was determined. The structural solution was attained using direct methods [*EXPO*2004 (Altomare *et al.*, 2004)], and located the two independent molecules in the asymmetric unit. The quality of the crystalline sample and the excellent diffraction data attainable at beamline ID31, ESRF, allowed a detailed structural characterization of the compound. VASP theoretical calculations confirmed the correct characterization of the structure.

We thank beamline ID31, ESRF, for providing synchrotron radiation beam-time, the CDCHT-ULA (Subvention C-1511-07-B) and the FONACIT (Project LAB-97000821 and Subvention-200500703). We thank James A. Kaduk of INEOS Technologies for performing the VASP calculation.

## References

Albov, D. V., Rybakov, V. B., Babaev, E. V. & Aslanov, L. A. (2004). *Acta Cryst.* E**60**, o894–o895.
Allen, F. H. (2002). *Acta Cryst.* B**58**, 380–388.

Altomare, A., Caliandro, R., Camalli, M., Cuocci, C., Giacovazzo, C., Moliterni, A. G. G. & Rizzi, R. (2004). *J. Appl. Cryst.* **37**, 1025–1028.
Amitina, S. A., El'tsov, I. V., Rybalova, T. V., Gatilov, Yu. V. & Grigor'ev, I. A. (2004). *Russ. Chem. Bull.* **53**, 1700–1703.
Auld, D. S. (2001). *Handbook on Metalloproteins*, edited by I. Bertini, A. Sigel & H. Sigel, pp. 881–941. New York: Marcel Dekker, Inc.
Bordás, B., Sóhar, P., Matolcsy, G. & Berencsi, P. (1972). *J. Org. Chem.* **37**, 1727–1730.
Boultif, A. & Louër, D. (1991). *J. Appl. Cryst.* **24**, 987–993.
Brandenburg, K. (2001). *DIAMOND*, Version 2.1. Crystal Impact GbR, Bonn, Germany.
Castiñeiras-Campos, A., Ruiz-Amil, A., Martínez-Carrera, S. & García-Blanco, S. (1983). *Acta Cryst.* C**39**, 1094–1096.
Contreras, R. R., Fontal, B., Bahsas, A., Reyes, M., Suárez, T. & Bellandi, F. (2001). *J. Heterocycl. Chem.* **38**, 1223–1225.
Contreras, R. R., Fontal, B., Bahsas, A., Reyes, M., Suárez, T., Bellandi, F., Nava, F. & Cancines, P. (2005). *Rev. Latinoam. Quím.* **33**, 7–11.
Contreras, R. R., Fontal, B., Romero, I., Atencio, R. & Briceño, A. (2006). *Acta Cryst.* E**62**, o205–o208.
Costa, B. R. de, George, C., Li, G. & He, X. (1994). *J. Org. Chem.* **59**, 482–485.
Davidson, E. R. (1983). *Methods in Computational Molecular Physics*, Vol. 113, NATO Advanced Study Institute, Ser. C, edited by G. H. F. Diercksen & S.Wilson, p. 95. New York: Plenum Press.
Finger, L. W., Cox, D. E. & Jephcoat, A. P. (1994). *J. Appl. Cryst.* **27**, 892–900.
Fitch, A. N. (2004). *J. Res. Natl. Inst. Stand. Technol.* **109**, 133–142.
Gordon, A. J. & Ford, R. A. (1972). *The Chemist's Companion: A Handbook of Practical Data, Techniques and References*, pp. 429–437. New York: John Wiley and Son, Inc.
Griffin, J. F., Duax, W. L. & Weeks, C. M. (1984). *Atlas of Steroid Structure*, Vol. 2, pp. 3–22. New York: IFI/Plenum Data Company.
Halcrow, M. A. & Christou, G. (1994). *Chem. Rev.* **94**, 2421–2481.
Holm, R. H. & Solomon, E. I. (2004). *Chem. Rev.* **104**, 347–348.
Ianelli, S., Nardelli, M., Belletti, D., Jamart-Grégoire, B., Brosse, N. & Caubère, P. (1995). *Acta Cryst.* C**51**, 1838–1841.
Irngartinger, H., Altreuther, A., Sommerfeld, T. & Stojanik, T. (2000). *Eur. J. Org. Chem.* pp. 4059–4070.
Kain, W. & Schwederski, B. (1994). *Bioinorganic Chemistry: Inorganic Elements in the Chemistry of Life*, pp. 172–184. New York: Wiley.
Karlin, K. D., Kaderli, S. & Züberbühler, A. D. (1997). *Acc. Chem. Res.* **30**, 139–147.
Kostermans, G. B. M., de Wolf, W. H., Bickelhaupt, F. & Krever, M. (1987). *Rec. Trav. Chim. Pays-Bas*, **106**, 563–570.
Kresse, G. & Furthmuller, J. (1996). *Comput. Mater. Sci.* **6**, 15–50.
Kresse, G. & Hafner, J. (1993). *Phys. Rev. B*, **48**, 13115–13118.
Kresse, G. & Joubert, D. (1999). *Phys. Rev. B*, **59**, 1758–1775.
Larson, A. C. & Von Dreele, R. B. (2007). *GSAS*. Los Alamos National Laboratory, Los Alamos, New Mexico, USA.
Le Bail, A., Duroy, H. & Fourquet, J. L. (1988). *Mater. Res. Bull.* **23**, 447–452.
Malachowski, M. R., Adans, M., Elia, N., Rheingold, A. L. & Kelly, R. S. (1999). *J. Chem. Soc. Dalton Trans.* **13**, 2177–2182.
Mekhael, M. K. G., Bienz, S., Linden, A. & Heimgartner, H. (2004). *Helv. Chim. Acta*, **87**, 2385–2404.
Methfessel, M. & Paxton, A. T. (1989). *Phys. Rev. B*, **40**, 3616–3621.
Monkhorst, H. J. & Pack, J. D. (1976). *Phys. Rev. B*, **13**, 5188–5192.
Ohlbach, F., Gleiter, R., Oeser, T. & Irngartinger, H. (1996). *Liebigs Ann. Chem.* pp. 791–797.
Rietveld, H. M. (1969). *J. Appl. Cryst.* **2**, 65–71.
Roat-Malone, R. M. (2002). *Bioinorganic Chemistry*, pp. 187–228. New Jersey: Wiley-Interscience.
Schulze, B., Taubert, K., Gelalcha, F. G., Hartung, C. & Sieler, J. (2002). *Z. Naturforsch. B Chem. Sci.* **57**, 383–392.
Senge, M. O., Vicente, M. da G. H., Parkin, S. R., Hope, H. & Smith, K. M. (1992). *Z. Naturforsch. B*, **47**, 1189–1202.
Sheldrick, G. M. (2008). *Acta Cryst.* A**64**, 112–122.
Smith, G. S. & Snyder, R. L. (1979). *J. Appl. Cryst.* **12**, 60–65.
Solomon, E. I., Szilagyi, R. K., DeBeer, G. & Basumallick, L. (2004). *Chem. Rev.* **104**, 419–458.
Spek, A. L. (1990). *Acta Cryst.* A**46**, C34.
Stephens, P. W. (1999). *J. Appl. Cryst.* **32**, 281–289.
Thompson, P., Cox, D. E. & Hastings, J. B. (1987). *J. Appl. Cryst.* **20**, 79–83.
Toby, B. H. (2001). *J. Appl. Chem.* **34**, 210–213.
Weeks, C. M., Duax, W. L., Finnegan, R. A., Delecki, D. J. & Kojić-Prodić, B. (1984). *Acta Cryst.* C**40**, 1376–1378.
Wolff, P. M. de (1968). *J. Appl. Cryst.* **1**, 108–113.
Zhang, D., Xu, Y., Koh, L. L., Lam, Y. L. & Huang, H. H. (1993). *Acta Cryst.* C**49**, 1002–1007.